2

Theoretical Aspects of the Equilibrium State of Chain Crystals

Jens-Uwe Sommer

Institut de Chimie des Surfaces et Interfaces (ICSI-CNRS), 15 rue Jean Starcky, P.B. 2488, F-68057 Mulhouse, France. Present address: Leibniz-Institut of Polymer Research, Hohe Strasse 6, Dresden, Germany

Abstract. The equilibrium state of polymer single crystals is considered by explicitly taking into account the amorphous fraction formed by loops and tails of the chains. Using ideal chain statistics, a general expression for the free energy excess of the amorphous part is derived. I show that tight loops and close reentries are favored under experimental conditions for under-cooling of polymer single crystals. For many chain crystals, I show that the lamellar thickness increases with the number of chains in the crystal, and that extended chain conformations are thermodynamically favored when the number of chains in the crystal is sufficiently large. The role of finite bending rigidity of chains is discussed for folded chain crystals, as well as tilt effects in extended chain crystals.

2.1 Introduction

Since the discovery of folded chain crystals [1–3] polymer crystals are considered as meta-stable systems which properties are controlled by kinetic effects [4,5]. This point of view is supported by many observations, such as the spontaneous thickening of lamellae [6], the dependence of the melting behavior on the thermal history of bulk samples [7], and spontaneous morphological transformations as observed in thin films [8,9]. Moreover, true thermodynamic coexistence is not observed in polymers, the crystallization temperature being generally lower than the melting temperature. The under-cooling necessary to obtain polymer crystals under laboratory conditions can be as large as 100 K. Furthermore, it is commonly believed that equilibrium forms of polymer crystals consist of extended chains and that such (usually extraordinary thick lamellae) are usually not observed under experimental conditions. Exceptions are short chains such as n-Alkanes [10] and polyethylene (PE) under high external pressure [11].

In contrast to crystals formed by small molecules, the positions of the individual monomers in polymer crystals are restricted due to their connectivity, and the polymer chain as a whole has to undergo a transition from the

J.-U. Sommer: *Theoretical Aspects of the Equilibrium State of Chain Crystals*, Lect. Notes Phys. **714**, 19–45 (2007)
DOI 10.1007/3-540-47307-6_2

random coil (high entropy) state to a partially folded or extendend (low entropy) state. Thus, viewed on the scale of individual chains, the crystallization transition involves an *internal transition of the molecule* itself. This causes a kinetic barrier as the chain has to be rearranged into the ordered conformation, a process which bears some similarity to the folding transition of protein molecules [12]. However, in contrast to proteins which are supposed to attain their stable ground state within a short time, polymer crystals get trapped in meta-stable states. Using this paradigm, attention has focused on the understanding of the kinetical effects during the formation of chain crystals far away from equilibrium states [13].

On the other hand, not much attention has been paid to a thorough mathematical description of the equilibrium state of polymer single crystals. This involves the calculation of the free energy excess of the amorphous part formed by loops and tails of the chains. In the past there were attempts to explain properties of crystalline polymers with equilibrium concepts addressing the coexistence of crystalline and amorphous phases in the semi-crystalline state [14], in particular aimed to explain their broad melting behavior, see [15], as well as the phenomena of partial reversible melting [16, 17]. Recently, this issue has been raised again by Muthukumar [18] who emphasized the possibility of folded chain states as the equilibrium form of polymer single crystals. His approach has been originally addressed to crystals formed by single chains as they can be studied in computer simulations [19, 20]. Here, the extended chain form can be trivially excluded.

In this work, I consider several aspects of the equilibrium state of polymer single crystals using the model proposed by Muthukumar which will be extended to multi-chain crystals. In particular I will show that extended chain crystals are the equilibrium form for many chain crystals if sufficiently many chains are accessible and I will give a simple argument for their thermodynamic stability with reference to folded chain crystals. Furthermore, the role of finite flexibility of chains is discussed as well as the tilt of stems in extended chain crystals.

2.2 Thermodynamic Considerations about the Equilibrium Shape of a Polymer Single Crystal

Throughout this work the free energy of chain segments will be defined with respect to their value in an amorphous unrestricted chain in the melt phase, i.e. the free energy is expressed as the difference to that of the liquid phase. Using the approximation of Gaussian statistics for individual chains in the melt phase, the free energy per segment can be written as $-kT \ln c$, where c denotes the number of states available for the segment in a free chain. In the following, we take the statistical segment of length b as the basic unit of the chain.

For an infinitely extended crystal, we denote the latent heat of fusion per statistical segment by ϵ_0. Let us now consider the free energy of a segment, ϵ, at a temperature T below the melting temperature T_0. In a first order thermodynamic approximation, we obtain

$$\epsilon = \frac{\epsilon_0 \Delta T}{T_0} \ , \tag{2.1}$$

with

$$\Delta T = T_0 - T \ . \tag{2.2}$$

This approximation can be improved for larger under-cooling by the following expression [16, 21]

$$\epsilon = \frac{\epsilon_0 \Delta T T}{T_0^2} \ . \tag{2.3}$$

As an example, we consider polyethylene (PE) where the heat of fusion per mol of CH2-units is about 4.11 kJ. Taking a statistical segment formed by 6 chemical units, we obtain $\epsilon_0 = 4.1 \cdot 10^{-20}$ J. Using $T_0 = 414$ K and $T = 300$ K in Eq. (2.3) yields $\epsilon \simeq 0.8 \cdot 10^{-20}$ J which corresponds to about 2 kT. This gives us an orientation for the values of ϵ in the experimental relevant range of under-cooling.

In a next step, we consider the finite size of a single crystal formed by μ crystalline stems (oriented orthogonal to the cylinder cross-section) each comprising m statistical segments, as sketched in Fig. 2.1. The excess free surface energy of the amorphous fraction (loops and tails) is denoted by σ_f. For simplicity, we use the term "surface tension" instead of the term "excess surface free energy" in the following. Furthermore, we assume a spherical shape of the cylinder cross-section. The latter property, however, agrees rather nicely with recent simulations of single chain crystals [20]. The free energy can be written as

$$F = -\mu m \epsilon + 2\mu\sigma_f + \sigma\sqrt{\mu} m \ , \tag{2.4}$$

where $\sigma = 2\sqrt{\pi}\sigma_e$ represents lateral surface tension of the lamella and σ_f denotes the surface tension of the fold surface.

With the condition

$$N \simeq \mu m = \text{const} \ , \tag{2.5}$$

we obtain

$$F = -N\epsilon + N\sigma \frac{1}{\sqrt{\mu}} + 2\mu\sigma_f \ . \tag{2.6}$$

The equilibrium solution is readily obtained:

$$\mu^* = N^{2/3}\alpha \tag{2.7}$$

$$m^* = N^{1/3}/\alpha \ . \tag{2.8}$$

Here, I have introduced the *shape factor* α given by

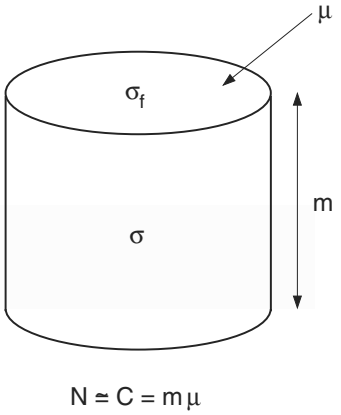

Fig. 2.1. Cylinder model for the single crystal. The cross-section contains μ crystalline stems of length m. The (tight) folds and ends are comprised in an excess free energy σ_f. Almost all monomers are considered to be contained in the crystalline fraction

$$\alpha = \left(\frac{\mu}{m^2}\right)^{1/3} = \left(\frac{\sigma}{4\sigma_f}\right)^{2/3} . \tag{2.9}$$

Note that this solution corresponds to Wulff's construction for the equilibrium shape of a cylindrical crystal [22].

In the above consideration, the surface tension, σ_f, has been introduced *ad hoc*. Its measurement is non-trivial since equilibrium crystals are usually extended chain crystals with a large lateral extension, i.e. $\mu \gg \mu^*$, so that the shape factor cannot be directly obtained. Usually, the value for σ_f is inferred from the melting line of the non-equilibrium crystal according to a Gibbs-Thompson approach, see [14]. I note that in this case neither the surface tension can be truly assumed to be an equilibrium property, nor can the validity of the Gibbs-Thompson extrapolation be tested independently. For a criticism of the Gibbs-Thompson approach for non-equilibrium polymer crystals, see [23].

It is therefore desirable to calculate the contribution of σ_f from equilibrium models which will provide more insight into the nature of the amorphous fraction. Clearly, we are restricted here to simplified models for the chain and the crystal part. As a first step, a two-phase model for the single crystal has to be introduced, which is illustrated in (Fig. 2.2). Segments can be exchanged freely between the crystalline (C) and the amorphous fraction (A) by conserving the total number of segments:

$$N = C + A = \text{const} , \tag{2.10}$$

Than, Eq. (2.4) can be generalized to

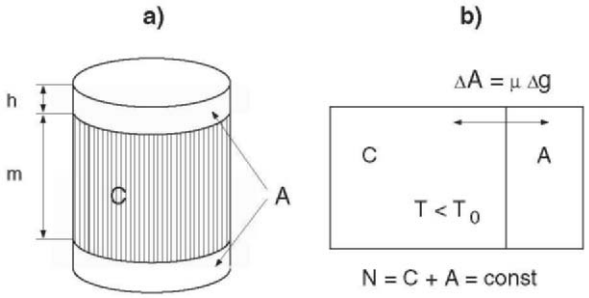

Fig. 2.2. Two-phase model for a cylindrical polymer crystal. (**a**) Loops and tails are explicitly considered as an amorphous fraction in thermodynamic equilibrium with the crystalline fraction. The height of the amorphous layers is denotes by h, keeping the notation for m as the length of the crystalline stems. Both length scales are considered in units of statistical segments. (**b**) Illustration of the thermodynamic equilibrium system. Segments can be exchanged between two phases and the temperature is considered to be lower than equilibrium melting temperature

$$F = -\mu m\epsilon + \sigma\sqrt{\mu}m + F_a = F_c + F_a \ , \tag{2.11}$$

where F_a denotes the free energy of the amorphous fraction with respect to the state of free chains and F_c represents the free energy of the crystalline fraction as discussed above. In the following, I will outline tractable statistical mechanical models for the amorphous fraction to understand the origin of the fold surface tension in equilibrium crystals.

2.3 The Brush State of the Amorphous Fraction is Thermodynamically Suppressed

Let us assume that the amorphous fraction forms a dense layer with an average loop length of $g \gg 1$ segments on either side of the crystal, and that the surface is sufficiently extended to obtain a homogeneous density of segments c_A in the amorphous fraction. Then, the height of the amorphous layers, see Fig. (2.2) is given by

$$h = \frac{g}{2}\left(\frac{1}{c_A\xi^2}\right) \sim g \ , \tag{2.12}$$

where the distance between the crystalline stems is denoted by ξ which corresponds to a crystallographic value of a few Å. The relation $h \sim g$ corresponds to a brush-like state where the loops and tails are extended in the direction perpendicular to the surface. Using a scaling approach [24], the free energy per loop can be written as

$$F_g \sim kT\left(\frac{h}{bg^{1/2}}\right)^2 \sim g \ , \tag{2.13}$$

where we have used Eq. (2.12), and b denotes again the length of a statistical segment. Thus, we can write $F_g = rkTg$, with a numerical constant r and the free energy of the brush-decorated crystal can be written as

$$F = \mu rkTg + \mu\epsilon g - \epsilon N + \sigma\sqrt{\mu}(N/\mu - g) \ . \tag{2.14}$$

The third term in this expression is the free energy of a crystal without an amorphous fraction. The free energy excess of the amorphous part is dominated by the first two terms which are both strictly positive. The first term corresponds the effort for stretching the chains in the brush state while the second term corresponds to the increase of free energy by pulling g segments out of the crystalline phase. Thus, under equilibrium conditions, where g is a variational parameter, the stable solution corresponds to the absolute minium of g which is possible to form a loop conformation. I note that the correction due to lateral surface tension (last term in Eq. (2.14) is also positive for $\sqrt{\mu} > \sigma/(rkT + \epsilon)$ which corresponds to a small number of stems. This calculations clearly demonstrate that a dense layer of long loops (and tails) does not correspond to a stable equilibrium state of the polymer crystal. In particular the brush-like state merely adds a free energy of several kT to each loop or tail which is transformed into the amorphous phase.

It is interesting to add that also individual chain tails are not favored thermodynamically. Here, we simply obtain

$$F = \gamma\mu\epsilon g - \epsilon N + \sigma\sqrt{\mu}(N/\mu - \gamma g) \ , \tag{2.15}$$

where faction of long loops/tails is given by $\gamma \ll 1$. Again, there is no stable solution for finite value of g, if the lateral extension of the crystal is not too small ($\sqrt{\mu} > \sigma/\epsilon$). This result is easy to understand: An isolated loop/tail with $g \gg 1$ just increases the free energy by a value of $g\epsilon$ without any compensation as referred to the equilibrium amorphous state.

2.4 Extended Chain Crystals and Sliding Entropy

In the section above we have tacitly assumed that the anchor points of the loops and tails are fixed. However, the possibility to distribute the amorphous segments in all possible ways along a given chain will give rise an an addition entropy as compared to the liquid state.

Let us consider a laterally infinitely extended polymer crystal. Each (extended) chain of length N_{ch} is composed of a (central) crystalline part made of m segments enclosed by $g = N_{ch} - m$ amorphous segments, which is illustrated in (Fig. 2.3). Since the crystalline part can be located anywhere along the chain this corresponds to a *sliding entropy* of

$$S_{slide} = k \ln g \ , \tag{2.16}$$

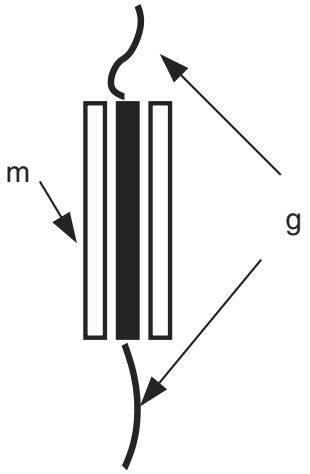

Fig. 2.3. Single chain within an extended chain crystal. Sliding of the chain trough the crystal phase (comprising m monomers per chain) is possible if g monomers are placed in the amorphous phase

where a constant S_0 can be suppressed. Thus, the free energy of a single chain in the extended chain crystal can be written as

$$F_{ext} = -kT \ln g + \epsilon g - \epsilon N_{ch} \ . \tag{2.17}$$

Minimization of Eq. (2.17) yields the equilibrium fraction of amorphous monomers per chain:

$$g_e = \frac{kT}{\epsilon} \ . \tag{2.18}$$

If we remember our example of PE given in section (2.2), we would obtain a small value of g_e. However, extended chain crystals can be observed rather close to the equilibrium melting temperature, where ϵ can become only fractions of kT. Using Eq. (2.3), we obtain

$$g_e = \frac{kT_0^2}{\epsilon_0 \Delta T} \ . \tag{2.19}$$

The nominator leads to a divergency of g_e when approaching T_0 [1]. A similar effect has been already discussed by Fischer [16] and Zachmann [15] in the context of equilibrium pre-melting in semi-crystaline polymers.

[1] For short chain crystals such as obtained for n-Alkanes, the equilibrium melting temperature T_0 must be replaced be maximum equilibrium melting temperature corresponding to the finite thickness of the crystals for $m = N_{ch}$. This takes into account a certain melting point depression due to the bare surface tension of the top and bottom surface.

However, Eqs. (2.18) and (2.19) are only valid for moderate values of g_e. Large values lead to the brush state in the amorphous fraction where the logarithmic entropy gain due to sliding is quickly compensated by the linear penalty term due to chain stretching, see Eq. (2.13). Taking into account Eqs. (2.13) and using the same symbols as in Eq. (2.14), we obtain

$$g_e = \frac{kT}{\epsilon + rkT} \ , \tag{2.20}$$

which regulates the divergency for $\epsilon \to 0$. On the other hand, the crystal can avoid part of the stretching free energy by tilting the stems thus increasing the distance between stems projected onto the top and bottom surfaces. This issue will be discussed in Sect. 2.9.

In the above consideration I have neglected the surface tension of the lateral surfaces by assuming an infinitely extended crystal. In many experimental situations where extended chain crystals are studied, this approximation is justified since the lateral extension can be orders of magnitude larger than the height of the crystal. The free energy for finite crystal with the shape factor α, see Eq. (2.9) is given by

$$F = \alpha^3 m^2 F_{ext} + \sigma \alpha^{3/2} m^2 \ . \tag{2.21}$$

For $\alpha \ll 1$, the second term dominates the free energy of the crystal, and the chain must obtain a folded conformation. An extreme case being a crystal formed by a single chain only, where the extended conformation can not be stable at all, since no crystalline bonds can be formed.

An interesting question arrises of how many chains are necessary to make the extended chain form the stable solution. The above considerations suggest $\alpha \simeq 1$. For $m \gg 1$ and $g \ll m$ (the latter is again related to the avoidance of the brush state) we have $m \simeq N_{ch}$ and the number of chains necessary for the extended chain form is given by $n_{ext} \simeq N_{ch}^2$. Using a more rigorous approach, I will show further below that this results is qualitatively correct.

2.5 The Slip-Loop Model for the Entropy of the Amorphous Fraction of a Single Chain Crystal

In the last section I have shown that sliding of chains yields to an additional entropy which favors a finite fraction of amorphous tails. This idea can be generailzed to folded chain conformations as sketched in (Fig. 2.4). Here, I will consider a crystal made of a single chain.

The essential idea is to assume that *all segments of the amorphous part can be distributed in all possible ways among the various loops and tails* for a given stem length m and for a given number of stems μ. The equilibrium solution is than obtained by minimizing the resulting free energy with respect to both variables. This shall be denoted as the *slip-loop model*.

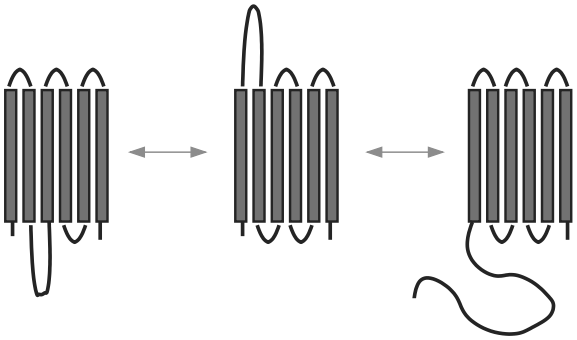

Fig. 2.4. Sketch of the slip-loop model for the amorphous part. The segments in the amorphous fraction can be arbitrarily distributed among the $\mu - 1$ loops and the both tails

In order to proceed, I have to make some assumptions about the chain statistics and about the form of the crystal. The latter should be given again by the model sketched in (Fig. 2.2). In particular, all stems should have the same length. To start with a tractable model, I will further ignore excluded volume interactions between the segments of the amorphous fraction as well as the conformational constraints due to the impenetrable crystalline surface. Furthermore, I treat the chain statistics as Gaussian and ignore effects of finite flexibility of the chain. These relaxed conditions overestimate the entropy of the amorphous fraction. I will reconsider these approximations in the context of the exact solution for the idealized model.

The number of conformations available for a Gaussian chain with g segments starting at $\boldsymbol{r}_0$ and ending at $\boldsymbol{r}$ with respect to the free unconstrained chain is given by

$$G(\boldsymbol{r}_0, \boldsymbol{r}; g) = \left(\frac{1}{4\pi l^2 g}\right)^{3/2} \exp\left(-\frac{(\boldsymbol{r} - \boldsymbol{r}_0)^2}{4l^2 g}\right) \Delta v \ , \tag{2.22}$$

with $l^2 = b^2/6$. The factor Δv compensates for the formally infinitely sharp localization of the end-segment of the chain in a continuous space and denotes the uncertainty of the localization of the end-segment. The physical meaning of this factor will be discussed further below. We call $G(\boldsymbol{x}, \boldsymbol{x}'; g)$ the Green function. The free energy difference of the restricted chain with respect to a free chain is than given by $F = -kT \ln G$ which corresponds to my notation of the free energy in this work. The mathematical task is completed if the Greensfunction of the amorphous part G_a has been calculated.

The contribution of the tails can be explicitly taken into account, since each tail just provides $G_t = 1$ (integration of Eq. (2.22) over $\boldsymbol{r}/\Delta v$). This yields

$$G_a(A) = \int_0^A dn (A - n) G_L(n, \mu - 1) \ , \tag{2.23}$$

where G_L denotes the contribution from loops only. Note that the contribution to Eq. (2.23) is only due to the various positions the loop part, made of n segments, can take within the amorphous part made of A segments. The details of the calculation of the loop part is more technical and can be found in Appendix A. The result is given by

$$G_L(A,\mu-1) = \frac{1}{\kappa^{\mu-1}}\sqrt{\frac{(\mu-1)\xi^2}{4\pi A l^2}}\frac{1}{A}\exp\left\{-\frac{(\mu-1)^2\xi^2}{4Al^2}\right\} \ . \tag{2.24}$$

Here, I have introduced the dimensionless *localization parameter*

$$\kappa = 4\pi l^2\xi/\Delta v \ , \tag{2.25}$$

where ξ characterizes the minimal distance between the loop ends, see also Sect. 2.3. Note the similarity between Eq. (2.24) and the single chain result of Eq. (2.22). Using Eq. (2.23) the final solution reads

$$G_a(A,\mu) = \frac{4A}{\kappa^\mu}\cdot\left[\left(\frac{1}{4}+\frac{1}{2}y\right)\mathrm{erfc}(\sqrt{y}) - \frac{\sqrt{y}}{2\sqrt{\pi}}\mathrm{e}^{-y}\right] = \frac{4A}{\kappa^\mu}\cdot f(y) \ , \tag{2.26}$$

where I have introduced the *scaling variable* y, defined by

$$y = \frac{(\mu-1)^2\xi^2}{4Al^2} \tag{2.27}$$

and $\mathrm{erfc}(y)$ denotes the complimentary error function ($\mathrm{erfc}(y) = \frac{2}{\sqrt{\pi}}\int_y^\infty dx\mathrm{e}^{-x^2}$).

In the following I consider only the case $\mu \gg 1$, which is the physical relevant solution for single chain crystals. The scaling variable can be related to the *average loop length* in the amorphous fraction

$$g = \frac{A}{\mu} \ . \tag{2.28}$$

by

$$y = \frac{a}{kT}\frac{\mu}{g} \ , \tag{2.29}$$

where

$$a = \frac{3}{2}kT\left(\xi/b\right)^2 \ . \tag{2.30}$$

denotes the maximal energy of the Gaussian spring which is formed by a single loop. The scaling variable y thus denotes the spring energy in units of kT related to μ loops, containing g segments each. Assuming an average free energy per loop of the order of kT, we can conclude that the physical relevant case is given by

$$y \gg 1 \ . \tag{2.31}$$

The opposite case of $y \ll 1$ can only be realized if the average loop length is very large ($g \gg \mu$). The latter must be excluded in order to avoid the brush

regime. However, Eq. (2.31) can also be justified without referring the brush regime. Generally, we obtain from Eq. (2.27)

$$A \sim \mu^2 \quad \text{for} \quad y \sim 1 \; . \tag{2.32}$$

The free energy effort to transfer A segments into the amorphous state is given by $\epsilon A \sim \mu^2$. I will show below that the solution for the case $y \gg 1$ leads to a surface excess which scales proportional to μ only.

Using Eqs. (2.26) in the limiting case (2.31), the free energy of the amorphous fraction can be written as

$$F_a = -kT \ln G_a = \mu \left(2\sigma_{f0} + \frac{a}{g} \right) \quad \text{for} \quad y \gg 1 \quad \text{and} \quad \mu \gg 1 \; , \tag{2.33}$$

with

$$2\sigma_{f0} = kT \ln \kappa \; . \tag{2.34}$$

For details, see Appendix B.

The localization parameter κ, see Eq. (2.25), can be related to the entropic restriction of an anchoring segment compared to a segment in a free chain. I will therefore consider κ as the ratio of the number of states of the end segments in the free chain compared to the anchored state. In a rough approximation the segments which directly anchor to the crystalline stem loose about half of the degrees of freedom being restricted to the half space. Therefore, the anchoring contribution might be estimated as $\kappa \simeq 2$ for each anchored segment. The corresponding free energy contribution per stem is thus comparable to kT. This free energy excess gives rise to an *entropic* surface tension, σ_{f0}, which increases with temperature.

I note that the solution in Eq. (2.33) is equally obtained using the loop part only, see Eq. (2.24). This indicates that tails do not play an singular role.

2.6 Tight Loops and Effective Fold Surface Tension for Single Chain Crystals

Using Eq. (2.11) we get for the free energy of the single chain crystal

$$F = F_c + F_a = -\mu m \epsilon + \sigma \sqrt{\mu} m + \mu \left(2\sigma_{f0} + \frac{a}{g} \right) \; . \tag{2.35}$$

The state of thermodynamic equilibrium is given by the minimum of F with respect to μ, g and m under the constraint of Eq. (2.10). A solution can be obtained analytically for $N \gg 1$, which is the physically relevant case. The direct solution of the minimization problem is given in Appendix C.

However, the solution presented in Appendix C can be rederived using a simple argument which reveals the essential physics most clearly. For $N \gg 1$, we disregard the lateral surface tension and assume that the optimal value

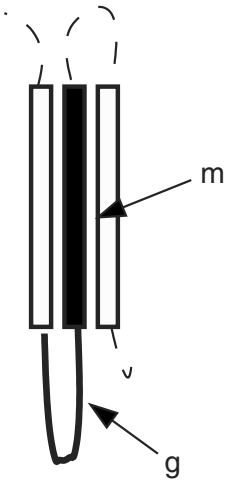

Fig. 2.5. Sketch of a single loop-stem element in the crystal

of g can be obtained by minimization for a single stem-loop element which is sketched in Fig. 2.5. The corresponding free energy reads

$$F_{sl} = 2\sigma_{f0} + g\epsilon + \frac{a}{g} = 2\sigma_{f0} + g\epsilon + \frac{3}{2}kT\frac{(\xi/b)^2}{g} \ . \tag{2.36}$$

Here, the second term is attributed to the transition of g monomers into the disordered phase and the third term represents the g-dependent part of the free energy from Eq. (2.33) related to a single loop. This latter part, however, agrees exactly with the free energy stored in a loop of g segments with the end-to-end separation of ξ. Thus, the essential free energy balance is between melting a segment and the corresponding decrease of the free energy of a Gaussian spring which is prolongated by one segment. Minimization of F_{sl} with respect to g gives

$$g_0^2 = \frac{a}{\epsilon} = \frac{3}{2}\frac{\xi^2}{l^2}\frac{kT}{\epsilon} \ , \tag{2.37}$$

which agrees with the solution for the full minimization problem given in Appendix C. According to our discussion in Sect. 2.2, the value of ϵ is not expected to become very small under usual experimental conditions. Therefore, the solution above indicates the formation of tight loops. Physically speaking, g_0^2 represents the ratio between the maximum free energy of the Gaussian spring to the free energy loss by pulling a segment out of the crystaline phase.

Being at the limit of validity, the Gaussian statistics used so far has to be scrutinized. This concerns in the first place the effect of finite bending rigidity which involves a fine-graining of the model towards a length scale smaller than the statistical segment length. I will come back to this issue in Sect. 2.8. On the other hand, for equilibrium crystals it should be possible (at

least theoretically) to consider also small values of ϵ thus approaching close to the equilibrium melting point. In this case, g_0 can become sufficiently large to justify the Gaussian statistics.

Using the result of Eq. (2.37), we obtain for the minimal free energy excess per loop of the amorphous fraction

$$F_{sl} = F_{sl} = 2\sigma_{f0} + g_0\epsilon + \frac{a}{g_0} = 2\sigma_{f0} + 2\sqrt{\epsilon a} = 2\sigma_f \ , \tag{2.38}$$

where I have introduced the *effective fold surface tension* σ_f defined as

$$\sigma_f = \sigma_{f0} + \sqrt{a\epsilon} \ . \tag{2.39}$$

The optimal shape is now easily derived from the free energy of the single crystal taking into account the lateral surface tension

$$F = -\epsilon N + 2\mu\sigma_f + \sigma\sqrt{\mu}m \ . \tag{2.40}$$

The relation between m and μ is given by $m + g_0 = N/\mu$. For $m \gg 1$, we can disregard the difference between m and N/μ, and we are let to the effective one-phase approach of Eq. (2.4). The shape factor is given by

$$\alpha = \left(\frac{\sigma}{4\sigma_f}\right)^{2/3} = \left(\frac{1}{4}\frac{\sigma}{\sigma_{f0} + \sqrt{a\epsilon}}\right)^{2/3} \ . \tag{2.41}$$

Thus, we obtain the equilibrium values of the extension of the single crystal:

$$\mu^* = N^{2/3}\left(\frac{1}{4}\frac{\sigma}{\sigma_{f0} + \sqrt{a\epsilon}}\right)^{2/3} \tag{2.42}$$

$$m^* = \frac{N}{\mu} - g_0 \simeq \frac{N}{\mu} = N^{1/3}\left(\frac{1}{4}\frac{\sigma}{\sigma_{f0} + \sqrt{a\epsilon}}\right)^{-1/3} \tag{2.43}$$

As I have shown, the origin for the finite amorphous fraction formed by the (prevailing) loops is due to the balance between the entropic spring force created by the finite separation of the anchoring segments on the one hand side and the effort to remove the loop segments from the thermodynamically preferred crystalline phase on the other side.

There is another interesting conclusion from our free energy argument concerning the value of ξ. In the calculation it was introduced as the smallest possible separation between the end points of the loops. This mathematical argument can now be supported by a physical argument: Since the entropy of a loop increases quadratically with the distance ξ, see Eq. (2.36), in thermodynamic equilibrium the smallest possible distance is favored. Thus, loops have the tendency to close, i.e. tight folds are preferentially formed by thermodynamic reasons.

2.7 Many Chain Crystals

The results obtained in the last section can be readily extended to the case of many chain crystals. As I have shown, the essential argument which leads to the equilibrium state of the amorphous fraction can be reduced to the free energy balance of a single loop. As far as the number of folds per chain is large, i.e. the role of tails is only minor, the result of Eq. (2.37) holds true also within many chain crystals. A formal mathematical analysis of this problem can be found in [25]. Given a crystal thickness of m (not yet optimized), the free energy for a single chain within the many chain crystal is given by

$$F_{ch} = -\epsilon N_{ch} + 2\sigma_f \frac{N_{ch}}{g_0 + m} \ , \tag{2.44}$$

where $\mu_{ch} = N_{ch}/(g_0 + m)$ can be replaced again by N_{ch}/m for $m \gg 1$. Then, the free energy for the overall crystal formed by n chains is given by

$$F = nF_{ch} + \sigma m\sqrt{\mu n} \ . \tag{2.45}$$

Introducing the total number of segments $N = nN_{ch}$, we obtain

$$F = -\epsilon N + 2\sigma_f \frac{N}{m} + \sigma\sqrt{Nm} \ , \tag{2.46}$$

an expression which is again fully equivalent to Eq. (2.4). The solution for the equilibrium thickness m^* then reads

$$m^* = (nN_{ch})^{1/3} \left(\frac{4\sigma_f}{\sigma}\right)^{2/3} \sim n^{1/3} \ . \tag{2.47}$$

This result tells us that the equilibrium thickness of the crystal is growing with the number of chains. Thus, at a certain point the thickness can become larger than the extension of the individual chains, and the extended chain crystal becomes the equilibrium form. With $m^* = N_{ch}$, I obtain

$$n_{ext} = N_{ch}^2 \alpha^3 \ . \tag{2.48}$$

Further thickening is hampered by additional surface tension which is created by stacking several chains in one stem. This result corroborates the conclusion obtained at the end of Sect. 2.4, where I have approached the problem from the opposite limit of extended chain crystals.

In order to appreciate the values calculated above, I consider the example of an extended chain crystals formed by PE under high external pressure [11]. A polymer chain of about 100,000 g/mol of molecular weight for PE corresponds to a value of $N_{ch} = 1000$. Using Eq. (2.48), the estimated number of chains necessary to reach the stretched state amounts to about 1,000,000. This corresponds to a lateral size of the crystal of a few hundred nanometers.

On the other hand, given the usual thickness of *non-equilibrium* PE crystals of the order of 10 nm, the same amount of chains require a lateral size of the order of a few micrometers which is within the experimentally observed range. Thus, non-equilibrium polymer single crystals can have the *potential* to form extended chain crystals in equilibrium.

The phase diagram for the equilibrium crystal is sketched in Fig. 2.6. If the number of chains, n, is increased, the thickness of the equilibrium crystal grows as the third root of n until it reaches the extended chain state at $n = n_{ext}$.

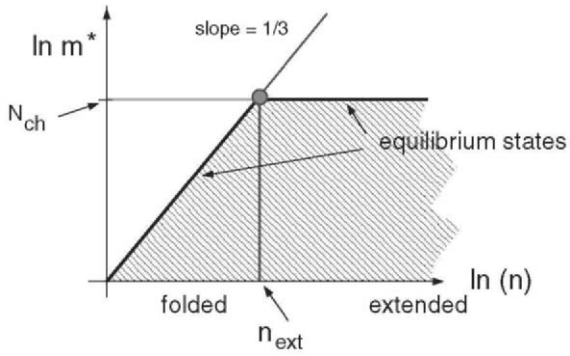

Fig. 2.6. Phase diagram of a polymer single crystal. The equilibrium states are indicated by the thick line. Non-equilibrium states (hatched area) are usually observed below the equilibrium line

When we approach the extended chain crystal, the approximation for the free energy of the amorphous fraction of the folded chain, Eq. (2.44), must be corrected to account for the dominating role of tails. This can be done using the full result for the free energy for the amorphous fraction, but the essential physics can be obtained in a much simpler way. In Sect. 2.4, the exact expression the free energy of an extended chain crystal has been derived. Here, only the tails contribute to the free energy of the amorphous fraction. In this case, only sliding of the chain (positioning of the crystal stem within the chain) is responsible for a finite amount of amorphous material per chain. By contrast, in case of folded chain crystals, the Gaussian spring energy of loops competes with the crystallization energy and the sliding term is reduced to a small contribution when many folds are formed. At the cross-over between both regimes, the amount of sliding entropy becomes increasingly important and eventually prevails the contribution from the loops. The transition is finally discontinuous because an integer number of folds have to be formed.

The only part which is left to prove is the stability of the extended chain form with respect to the folded chain form. This can be easily inferred from the following Gedankenexperiment as sketched in Fig. 2.7. Let us consider a single chain crystal formed by a huge chain of length N in thermodynamic

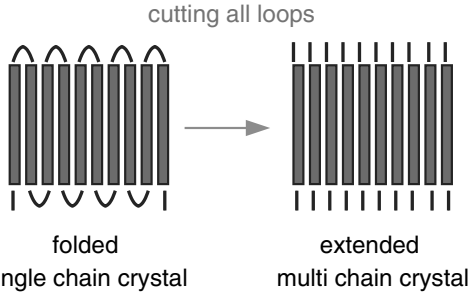

Fig. 2.7. An extended chain crystal is obtained by cutting all loops of a single chain, folded crystal

equilibrium with $\mu \gg 1$ and $m \gg 1$, see left part of Fig. 2.7. Then, we cut all loops and obtain a multi chain crystal formed by N/μ extended chains having the length of $N_{ch} = m + g_0$ monomers, see right part of Fig. 2.7. Note that N_{ch} can be arbitrary large, since $m \sim N^{1/3}$, see Eq. (2.43). The free energy change for the transition from the folded to the extended chain crystal is given by

$$\Delta F = \mu \left(-\frac{a}{g} - kT \ln g \right) \ , \tag{2.49}$$

which is *strictly negative*. The first term corresponds to the opening of the loops (release of Gaussian stretching free energy) and the second term corresponds to the fee energy gain due to the *independent* sliding motions of the individual stems as is has been derived in Sect. 2.4. Thus, the extended chain form is thermodynamically preferred, if the freedom to open chain loops is given.

The essential conclusion from this paragraph is that folded chain crystals are equilibrium forms only if the number of chains contained in the crystal is limited. Here, the extended chain form can violate the optimal crystal shape according to the Wulff construction.

2.8 The Role of Bending Rigidity for the Formation of Small Loops

So far, I have considered the Gaussian chain model based on coarse-graining on the scale of a statistical segment length. For folded chain crystals, the equilibrium loop length according to Eq. (2.37) turns out to be close to unity if experimental values for the under-cooling are considered. Such small loops, however, have to bear a considerable amount of bending energy and the Gaussian approximation is limited. In this section, I will discuss the effect of finite bending rigidity for a continuous chain model. This will address the situation of tight loops only where the Gaussian approach fails. The chain is described by the path $\boldsymbol{r}(s)$ parameterized by the arc length along the chain's contour.

The bending rigidity B of the homogeneous chain (*worm-like chain model*) is related to the statistical segment by [26]

$$B = 2kTb \ . \tag{2.50}$$

Then, the energy of a loop of length gb can be written as

$$E = kTb \int_0^{gb} ds \left(\frac{d\boldsymbol{t}(s)}{ds} \right)^2 \ , \tag{2.51}$$

where $\boldsymbol{t}(s) = d\boldsymbol{r}(s)/ds$ denotes the normalized tangent vector of the chain at position s. Here, g, denotes a real number which can be smaller than unity. For a loop-like conformation, one obtains

$$E = \zeta 4\pi^2 kT \frac{1}{g} \ , \tag{2.52}$$

where the constant ζ accounts for a non-trivial form of the loop. The value $\zeta = 1$ gives the result for a circle. The statistical weight to be taken into account for each loop can be thus written as

$$G_w(s) \sim \exp\left\{ -\frac{1}{4} \frac{a_0^2}{g} \right\} \ , \tag{2.53}$$

with

$$a_0^2 = 16\zeta\pi^2 \ . \tag{2.54}$$

Here, the index "w" reminds to the worm-like chain model. Note that this approach is only valid if fluctuations of the chain's contour are not dominating. Thus, it represents the complementary case to the Gaussian approach, were only fluctuation are taken into account.

Nevertheless, there is a strong similarity between the exponentials of Eqs. (2.53) and (2.22). To proceed, it is worth noting, that the essential part of the Laplace-transform which allows the calculation of the multiple integral for G_L, see Appendix A, is determined by a stationary point of the Laplace-integral only and hence (within this approach) the same result is obtained using G_{wl} instead of G. Thus, following the same steps as presented in Appendix A, the essential part of the free energy of the amorphous fraction can be written as

$$F_a = \mu \left(2\sigma_{f0} + \frac{a}{g} \right) \ , \tag{2.55}$$

where the constant a is now defined as

$$a = 4\zeta\pi^2 kT \ . \tag{2.56}$$

I note that the bare surface tension, σ_{f0}, has an empirical meaning only, although it must be still related to the localization of the end-points of the loop. In fact, being constant, σ_{f0} is not important for the physical most significant

conclusion about the average loop length. Mapping the redefinition of a onto the results obtained in Sect. 2.6, I get

$$g_0^2 = \frac{a}{\epsilon} = 4\zeta\pi^2 \frac{kT}{\epsilon} \ . \tag{2.57}$$

Comparing this result to Eq. (2.37), one can conclude that the equilibrium loop length is larger (in units of the statistical segment length), although a physical interpretation is now possible for g smaller than unity. Using reasonable estimates for PE at room temperature, see Sect. 2.2, a value for g_0 of the order of a few statistical segments (depending on the value of ζ) is predicted. This, however, means that even under such conditions, the *optimal loop length does not correspond to the absolute minimum* (given by the tightest fold which can be formed [4]), but may contain a few persistence lengths.

To conclude, the calculation using a worm-like chain model gives further evidence for the formation of small loops, but suggests that these loops are not necessarily limited by the chemical structure. This is easy to understand, since the free energy loss for pulling one segment out of the crystalline phase is only of the order of kT (or less) at experimental temperatures.

2.9 Tilting in Extended Chain Crystals

As I have shown in the previous sections, the equilibrium state of a polymer single crystal contains extended chains only, if sufficiently many chains are available. An interesting aspect in the calculation of Sect. 2.4 is the existence of a *positive* entropy related to the amorphous fraction due to the sliding of chains, see Eq. (2.16). This, however, is quickly balanced by the excluded volume interactions between the tails, as has been discussed in the context of Eq. (2.20).

Now, there is a possibility to reduce the effect of excluded volume interactions by tilting the crystal stems with respect to the top and bottom surface. This idea is illustrated in Fig. 2.8.a). The increase of surface area per chain is given by

$$\xi'^2 = \xi^2 / \cos\alpha \ , \tag{2.58}$$

where the tilting angle α is defined between the stem orientation and the normal to the interface between the crystaline and the amorphous phase. Using the scaling approach to the brush limit of Sect. 2.3, see Eqs. (2.12) and (2.13), the free energy contribution for a single chain with respect to the brush state can be written as

$$F_{brush} = kTg \frac{r}{(c_A v_0)^2} \cos^2\alpha \ , \tag{2.59}$$

where r denotes a constant which cannot be obtained from scaling. The symbol $v_0 = \xi^2 b$ denotes the segment volume as used for the derivation assuming a

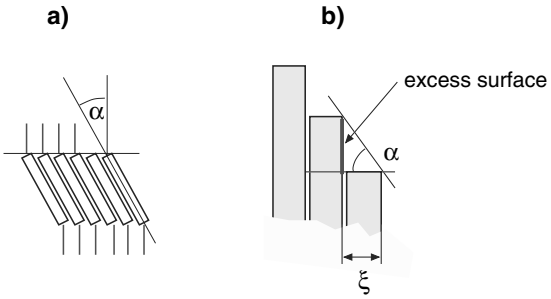

Fig. 2.8. Tilted extended chain crystal. (**a**) Tilted stems lead to a decrease of the grafting density of the tails. The angle α is defined between the stem orientation and the normal of the interface between the crystaline and the amorphous phase. (**b**) Tilting of stems increases the free energy by creating excess surface

dry brush state. Thus the product $c_A v_0$ should be close to unity. To abbreviate the notation, I introduce the constant $r' = r/(c_A v_0)^2$.

On the other hand, tilting gives rise to the formation of an excess surface per chain as illustrated in Fig. 2.8.b). The corresponding free energy excess per chain is given by

$$F_{exe} = 2s'\xi \tan\alpha \frac{\epsilon}{b} = 2s\epsilon \tan\alpha \ . \tag{2.60}$$

Note that the excess free energy (as well as the brush free energy) has to be taken on both sides of the crystaline fraction which gives rise to the factor of two. Here, I have assumed that the excess free energy is related due to a missing neighbor effect to the free energy difference ϵ, and s (s') denotes again a constant. In a more general approach, a surface tension σ_{exe} could be introduced instead of $s\epsilon$. By using $s\epsilon$ in Eq. (2.60), it is tacitly assumed that the excess surface tension vanishes if the system approaches the equilibrium melting point.

Using Eqs. (2.16) and (2.17), the total free energy per chain can be written as

$$F = F_{ext} + F_{brush} + F_{exe} = -kT \ln g + \epsilon g - \epsilon N_{ch} + kT g r' \frac{1}{1+q^2} + 2s\epsilon q \ , \tag{2.61}$$

with

$$q = \tan\alpha \ . \tag{2.62}$$

The minimization problem for F with respect to q and g can be solved in the limit of small values of ϵ and yields to

$$q^3 \simeq \frac{r'}{s} \left(\frac{kT}{\epsilon}\right)^2 \ . \tag{2.63}$$

Details can be found in Appendix D.

The second derivative of Eq. (2.61) with respect to q is given by

$$\frac{\partial^2 F}{\partial q^2} = \frac{2gkTr'}{(1+q^2)^3}(3q^2-1) \ . \tag{2.64}$$

Thus, a minimum for the free energy is impossible for angles below a critical angle α_c given by

$$\tan\alpha_c = \frac{1}{\sqrt{3}} \quad \text{and} \quad \alpha_c = 30^\circ \ . \tag{2.65}$$

Given the other approximations, this is valid as long as the scaling approach for F_{brush} holds. The latter condition will fail at larger under-cooling where g becomes very small. In order to estimate the temperature effect, the solution given by Eq. (2.63) shall be analyzed further. Using Eq. (2.3) leads to

$$q \simeq \frac{r'}{s}\left(\frac{kT_0}{\epsilon_0}\right)^{2/3} \Delta^{-2/3} \ , \tag{2.66}$$

where I have introduced the *dimensionless under-cooling*

$$\Delta = \frac{T_0 - T}{T_0} \ . \tag{2.67}$$

The first prefactor in Eq. (2.66) might be rather large because s is small, however, r' is unknown. The second prefactor, given by the latent heat of melting of a segment at the equilibrium melting point, takes a value of about 1/8 for PE.

Experimentally, tilting of chains in polymer crystals is well known. Recently, chain titling has been analyzed in annealing experiments of long n-Alkanes using FTIR and SAXS techniques by de Silva et al. [27, 28]. Here, the authors found irreversible tilting up to an angle of about $\alpha \simeq 35^\circ$ during annealing experiments. This is qualitatively explained as a perfectioning process of surface disorder [29] although the "overcrowing problem" has been noted by the authors. However, these crystals are usually grown under non-equilibrium conditions, and relaxation into the equilibrium state at rather low temperatures might be prohibited. It is interesting to note that the observed maximum tilt angle before melting is close to the critical angle predicted in Eq. (2.65). This might suggest that the irreversible tilting observed in these experiments are due to the meta-stability of the brush with respect to tilt. At this point, more experimental (and simulation) studies close to the melting point of extended chain crystals are necessary to understand the origin of chain tilt in short-chain crystals. The above presented arguments provide an alternative explanation for such effects and should be taken into account for the interpretation of experimental results.

2.10 Summary and Conclusion

In this work I have considered the equilibrium state of a polymer single crystal as a two-phase systems composed of a crystalline and an amorphous fraction.

A statistical mechanical model is used for the amorphous fraction taking into account the disorder in the distribution of monomers among the loops and tails. The major results of the analysis are summarized as follows:

- Folded chain crystals form equilibrium states only if the number of chains within the crystal is resticted.
- For folded chain crystals the average loops size in the amorphous fraction is determined by the balance between the Gaussian spring force (or bending rigidity) and the effort to transform a segment into the amorphous phase. The latter is of the order of kT under experimental conditions. Loops at the limit of a few statistical segments are likely to be formed.
- Extended chain crystals gain free energy due to chain sliding. Extended chain crystals are formed if an unrestricted number of chains is available.
- Titling of stems reduces excluded volume effects in the amorphous fraction close to the melting point.
- The equilibrium tilt angle increases with temperature. Small tilt angles are meta-stable.

These results rely on a number of assumptions. First, the Gaussian statistics of amorphous sequences does not properly account for the finite flexibility of chains (in case of tight loops). This aspect has been reconsidered explicitly using a model of finite bending rigidity. The obtained results suggest that the equilibrium loop length can be well above the statistical segment size thus the Gaussian approach is just on its limit. Excluded volume effects are explicitly discussed using a scaling approach for the free energy of a polymer brush.

Due to the presence of many tails and loops in the amorphous fraction the effect of half-space restriction is less important. Following Silberberg's argument [30] for a dense polymer system, the polymer-type *adsorbing* boundary condition [24, 26] should be replaced by a reflecting boundary condition. For the latter case, the surface represents a much weaker constraint. Moreover, there is another argument which relativizes the effect of the impenetrable surface: If the average length of amorphous sequences is short, bending rigidity is important. Since the sequences start perpendicular to the surface the probability of stochastic returns can be neglected. On the other hand, if sequences are longer, excluded volume interactions become important because of the high grafting density provided by the crystal packing of stems, and the sequences are stretched away from the surface. Thus, I'm let to the conclusion that entropic effects due to geometric restrictions of chains should not be dominant.

Another approximation made throughout this work is the assumption of a flat, non-fluctuating crystal surface. The stems in the crystalline phase are assumed to be of equal length and transitions between the crystaline fraction and the amorphous fraction occur instantanously. Here, two effects are disregarded: First, fluctuations of the stem length might decrease the free energy in a certain range of temperature, and second, a curved or tapered from of the crystal might become favorable. The latter argument seems to be tempting for

extended chain crystals where the free energy of the amorphous fraction can become very small (sliding entropy leads even to a negative contribution) and a tapered form might reduced the free energy be reducing the lateral surface tension. A closer analysis shows that a tapered shape would also induce an excess surface tension since neighboring stems have missing neighbor effects. This is in full analogy to the arguments used for tilting of chain in Sect. 2.9. A simplified calculation, following the idea of Sect. 2.9 for calculating the excess free energy, see also Fig. 2.8, leads to a flat surface with isolated steps. However, other possible effects should be considered for the formation of tapered forms such as the role of excluded volume interactions, in particular the effect of "overspilling" of tails close to the crystal boundary.

Only equilibrium states have been considered in this work. Many of the effects mentioned here, can be alternatively discussed in the context of non-equilibrium. On the other hand, the question arrises, whether the calculations presented here can be applied to meta-stable states of polymer crystals, in particular to the case of semi-crystalline polymers. In fact, similar arguments have been used in early works [15,16] to explain the melting behavior of semi-crystaline polymers. A few points should be taken in mind here. First, and in contrast to the equilibrium scenario, the loop lengths in non-equilibrium semi-crystalline systems will be distributed with a distribution determined by the growth process and the averaged loop length is not simply related to the equilibrium loop length discussed in this work. Second, when temperature is changed in non-equilibrium systems, relaxation effects are accelerated, such as thickening of lamellae [9], and unfolding of chains [27]. These generic non-equilibrium forces are superposed to the equilibrium-forces considered in this work.

The calculations presented in this work should serve as an alternative starting point for a deeper understanding of the coexistence between crystaline and amorphous phases in polymers. In particular, a closer inspection of the effect of finite flexibility and possible orientation dependent interactions between amorphous segments could lead to better understanding of the crystalline-amorphous interface which plays an important role in experimental analysis and applications of crystalline polymers.

I kindly acknowledge discussions with M. Muthukumar, A. Johner and G. Reiter.

Appendix A

The partition function for the loop part of the amorphous fraction is obtained by integrating over all possible distributions of individual loop lengths

$$G_L(n,\mu) = \int_0^n dg_\mu G(\Delta \boldsymbol{r}_\mu; n - g_\mu) \int_0^{g_\mu} dg_{\mu-1} G(\Delta \boldsymbol{r}_{\mu-1}; g_\mu - g_{\mu-1}) \cdots \\ \cdots \int_0^{g_2} dg_1 G(\Delta \boldsymbol{r}_1; g_2 - g_1) \ , \tag{2.68}$$

where $\Delta \boldsymbol{r}_k$ denotes the spatial distance between the both endpoints of the k^{th} loop. In order to simplify the calculation we assume a constant end-to-end distance for all loops

$$|\Delta \boldsymbol{r}_k| = \xi \ . \tag{2.69}$$

In adjacent folds the distance ξ corresponds to the lateral distance between the stems (the lattice constant a or b of the crystal). Hence, ξ can be considered as a small *cut-off* distance. It is essential to keep this distance non-zero – as it corresponds to reality. Otherwise, the integrals in Eq. (2.68) will diverge for $\Delta t_k \to 0$. As shown in Sect. 2.6, the equilibrium solution predicts the smallest possible value for ξ, which corresponds to adjacent folds.

Using the convolution theorem of the Laplace transformation we obtain

$$\hat{G}_L(p,\mu) = \hat{G}(\xi,p)^\mu \ , \tag{2.70}$$

where $\hat{G}(\xi,p)$ denotes the Laplace-transform of the Green function $G(\xi,g)$ with respect to the contour length variable. From Eq. (2.22) we obtain

$$\hat{G}_L(p,\mu) = \left(\frac{a_0 \Delta v}{4\pi l^3}\right)^\mu \mathrm{e}^{-\mu a_0 \sqrt{p}} \ , \tag{2.71}$$

with

$$a_0 = \xi / l \ . \tag{2.72}$$

Inverse Laplace transformation of Eq. (2.70) using (2.71) yields

$$G_L(n,\mu) = \frac{1}{\kappa^\mu} \frac{\mu a_0}{2\sqrt{\pi}} \frac{1}{n^{3/2}} \exp\left\{-\frac{\mu^2 a_0^2}{4n}\right\} \ , \tag{2.73}$$

which corresponds to Eq. (2.24) after substitution of (2.72).

Appendix B

Here, the limiting case $y \gg 1$ is considered for the result of Eq. (2.26). Using the leading term in the asymptotic expansion of the complementary error function we obtain

$$f(y) \simeq \frac{e^{-y}}{8z^3\sqrt{\pi}} \quad \text{for} \quad y \gg 1 \ . \tag{2.74}$$

Thus, the free energy for the amorphous fraction is given by

$$\begin{aligned} F_a &= kT\mu \ln \kappa - kT \ln A - kT \ln f(z) \\ &= 2\mu\sigma_{f0} - kT \ln(g\mu) + kTy + \frac{3}{2} kT \ln(y) \ , \end{aligned} \tag{2.75}$$

where Eq. (2.34) has been used. In the limiting case $y \gg 1$ and $\mu \gg 1$ both logarithmic terms can be disregarded, and using Eqs. (2.29) and (2.30) we obtain

$$F_a = \mu \left(2\sigma_{f0} + \frac{a}{g} \right) \ . \tag{2.76}$$

Appendix C

To solve the extreme value problem for the free energy given in Eq. (2.35) we introduce a Lagrange multiplier λ to fulfill Eq. (2.10). Using further the crystalline fraction as defined in (2.10) we obtain

$$F_\lambda = -C\epsilon + \frac{\sigma}{\sqrt{\mu}} C + \mu \left(\sigma_{f0} + \frac{a}{g} \right) - \lambda \left(N - C - g\mu \right) \ . \tag{2.77}$$

Minimization of F_λ with respect to the three parameters g, C and μ leads to the following three equations:

$$\lambda = \frac{a}{g^2} \tag{2.78}$$

$$\epsilon = \frac{\sigma}{\sqrt{\mu}} + \lambda \tag{2.79}$$

$$C = \frac{2\mu^{3/2}}{\sigma} \left(g\lambda + \left(\sigma_{f0} + \frac{a}{g} \right) \right) \ . \tag{2.80}$$

Additionally, Eq. (2.10) has to be satisfied. First, we obtain from Eqs. (2.78) and (2.79):

$$\mu = \left(\frac{\sigma g^2}{g^2\epsilon - a} \right)^2 \ . \tag{2.81}$$

Inserting Eq. (2.81) in Eq. (2.80) and using Eq. (2.10) we get

$$N = \left(\frac{\sigma g^2}{g^2\epsilon - a} \right)^3 \frac{1}{\sigma} \left[2\sigma_{f0} + \frac{3a}{g} + g\epsilon \right] \ . \tag{2.82}$$

It is now possible to obtain a solution of Eq. (2.82) for large values of N. There are two alternatives: First, g growths proportionally to N. This corresponds to $y \ll 1$ and has to be excluded, see Sect. 2.5. The second solution is given by very small values of $g^2\epsilon - a$ and corresponds to tight folds. For $N \to \infty$, the solution is

$$g_0^2 = \frac{a}{\epsilon} \ . \tag{2.83}$$

Appendix D

Minimization of Eq. (2.61) with respect to z and g yields to

$$\frac{q}{(1+q^2)^2} = \frac{E\delta}{g} \tag{2.84}$$

$$g = \frac{1}{E + \frac{r'}{1+q^2}} \ , \tag{2.85}$$

with

$$E = \frac{\epsilon}{kT} \quad \text{and} \quad \delta = \frac{s}{r'} \ . \tag{2.86}$$

The solution for q can be written as

$$q = \delta E^2 (1+q^2)^2 \left(1 + \frac{r'}{E}\frac{1}{1+q^2}\right) \ . \tag{2.87}$$

This equation can be solved iteratively for any value of r', δ and ϵ by starting at some value of q on the right hand side. As discussed in the text, see Eq. (2.64), the free energy is unstable with respect to the tilt angle for small values of q. Therefore, the possible solution $q \to 0$ for $\epsilon \to 0$ is unphysical.

The stable solution for small values of ϵ is thus given by large values of q, where the first approximation reads

$$q \simeq \delta E^2 q^4 \ , \tag{2.88}$$

which yields to Eq. (2.63). The self-consistency of this solution can be checked by substitution of Eq. (2.63) in Eq. (2.87).

References

[1] A. Keller. A note on single crystals in polymers – evidence for a folded chain configuration. *Phil. Mag.*, 2(21):1171, 1957.

[2] E. W. Fischer. Stufenförmiges und spiralförmiges wachstum bei hochpolymeren. *Z. Naturf. A*, 12(9):753–754, 1957.

[3] P. H. Till. The growth of single crystals of linear polyethylene. *J. Polym. Sci.*, 24(106):301–306, 1957.

[4] J. D. Hoffmann, G. T. Davis, and J. I. Lauritzen. *The Rate of Crystallization of Linear Polymers with Chain Folding*, volume 3, pp. 497–614. Plenum Press, treatise in solid state chemistry edition, 1976.

[5] D. M. Sadler. New explanation fro chain folding in polymers. *Nature*, 326:174–177, March 1987.

[6] M. Hikosaka, K. Amano, S. Rastogi, and A. Keller. Lamellar thickening growth of an extended chain single crystal of polyethylene. 1. pointers to a new crystallization mechanism of polymers. *Macromolecules*, 30(7):2067–2074, March 1997.

[7] M. Al-Hussein and G. Strobl. The melting line, the crystallization line, and the equilibrium melting temperature of isotactic polystyrene. *Macromolecules*, 35(5):1672–1676, February 2002.
[8] G. Reiter, G. Castelein, and J.-U. Sommer. Liquidlike morphological transformations in monolamellar polymer crystals. *Phys. Rev. Lett.*, 86(26):1918–5921, June 2001.
[9] J.-U. Sommer and G. Reiter. Morphogegesis of lamellar polymer crystals. *Europhys. Lett.*, 56(5):755–761, December 2001.
[10] G. Ungar, J. Stejny, A. Keller, and M. C. Whiting. The crystallization of ultralong normal paraffines – the onset of chain folding. *Science*, 229(4711):386–389, 1985.
[11] S. Rastogi, M. Hikosaka, H. Kawabata, and A. Keller. Role of mobile phase in the crystallization of polyetylene. 1. matastability and lateral growth. *Macromolecules*, 24:6384–6391, 1991.
[12] J. A. Subirana. Elucidation of chain folding in polymer crystals: Comparison with proteins. *Trends in Pol. Sci.*, 5(10):321–326, October 1997.
[13] K. Armistead and G. Goldbeck-Wood. Polymer crystallization theories. *Adv. Polym. Sci.*, 100:219–312, 1992.
[14] G. Strobl. *The Physics of Polymers*. Springer, Berlin, Heidelberg, N.Y., 2 edition, 1997.
[15] H. Zachmann. Der Eeinfluss der Konfigurationsentropie auf das Kristallisations- und Schmelzverhalten von hochpolymeren Stoffen. *Kolloid Z. Z. Polym.*, 216–217:180–191, 1967.
[16] E. W. Fischer. Das grenzflächenschmelzen der kristallite in teilkristallisierten hochpolymeren. teil i: Theoretische grundlagen. *Kolloid Z. Z. Polym.*, 218(2): 97–114, June 1967.
[17] W. Hu, T. Albrecht, and G. Strobl. Reversible surface melting of pe and peo crystallites indicated by tmdsc. *Macromolecules*, 32(22):7548–7554, 1999.
[18] M. Muthukumar. Molecular modelling of nucleation in polymers. *Phil. Trans. R. Soc. Lond. A*, 361:539–556, 2003.
[19] P. Welch and M. Muthukumar. Molecular mechanisms of polymer crystallization from solution. *Phys. Rev. Lett.*, 87(21):218302, November 2001.
[20] L. Larini, A. Barbieri, P. A. Rolla, and D. Leporini. Equilibrated polyethylene single-molecule crystals: molecular-dynamics simulations and analytic model of the global minimum of the free-energy landscape. *J. Phys: Condens. Matter*, 17(19):L199–L208, 2005.
[21] J. D. Hoffman. Thermodynamic driving force in nucleation and growth processes. *J. Chem. Phys.*, 29(5):1192–1193, November 1958.
[22] G. Wulff. On the question of speed of growth and dissolution of crystal surfaces. *Zeitschrift für Kristallographie und Mineralogie*, 34:449, 1901.
[23] J.-U. Sommer and G. Reiter. Crystallization in ultra-thin polymer films morphogenesis and thermodynamical aspects. *Thermochimica Acta*, 432(2):135–147, June 2005.
[24] P. de Gennes. *Scaling Concepts in Polymer Physics*. Cornell University Press, Ithaca and London, 1979.
[25] J.-U. Sommer. The role of the amorphous fraction for the equilibrium shape of polymer single crystals. *Eur. Phys. J. E*, 19, 413–422, 2006.
[26] M. Doi and S. Edwards. *The Theory of Polymer Dynamics*. Clarendon Press, Oxford, 1986.

[27] D. S. M. de Silva, X. B. Zeng, G. Ungar, and S. J. Spells. Chain tilt and surface disorder in lamellar crystals. a ftir and saxs study of labeled long alkanes. *Macromolecules*, 35(20):7730–7741, September 2002.

[28] D. S. M. de Silva, X. B. Zeng, G. Ungar, and S. J. Spells. On perpendicular and tilted chains in lamellar crystals. *J. Macromol. Sci.*, B42(3,4):915–927, May 2003.

[29] J.-P. Gorce and S. J. Spells. Ftir studies of conformational disorder: crystal perfecting in long chain n-alkanes. *Polymer*, 45(10):3297–3303, May 2004.

[30] A. Silberberg. Distribution of conformations and chain ends near the surface of a melt of linear flexible macromolecules. *J. Coll. Interface Sci.*, 90(1):86–91, November 1981.